

Article

Not peer-reviewed version

Stabilization Performance and Mechanism of the Gravelly Soil Stabilizer Prepared from Waste Foam Concrete

Jizhong Gan , Xiantao Liang , Yang Song , [Bingxu Chen](#) ^{*} , Dongsheng Liu , Wanzhi Cao , Danhua Chen

Posted Date: 7 April 2026

doi: 10.20944/preprints202604.0450.v1

Keywords: waste foam concrete; gravelly soil; soil stabilizer; freeze-thaw resistance



Preprints.org is a free multidisciplinary platform providing preprint service that is dedicated to making early versions of research outputs permanently available and citable. Preprints posted at Preprints.org appear in Web of Science, Crossref, Google Scholar, Scilit, Europe PMC.

Copyright: This open access article is published under a [Creative Commons CC BY 4.0 license](#), which permit the free download, distribution, and reuse, provided that the author and preprint are cited in any reuse.

Disclaimer/Publisher's Note: The statements, opinions, and data contained in all publications are solely those of the individual author(s) and contributor(s) and not of MDPI and/or the editor(s). MDPI and/or the editor(s) disclaim responsibility for any injury to people or property resulting from any ideas, methods, instructions, or products referred to in the content.

Article

Stabilization Performance and Mechanism of the Gravelly Soil Stabilizer Prepared from Waste Foam Concrete

Jizhong Gan ^{1,3,4}, Xiantao Liang ^{1,3,4}, Yang Song ^{1,3,4}, Bingxu Chen ^{1,2,*}, Dongsheng Liu ^{1,3,4} and Wanzhi Cao ^{1,3,4} and Danhua Chen ^{1,3,4}

¹ College of Civil Engineering, Northwest Minzu University, Lanzhou 730124, China

² Department of Civil Engineering, University of Science and Technology Beijing, Beijing, 100083, China

³ Gansu Key Laboratory of Green Engineering Materials and Low-carbon Construction, Lanzhou 730124, China

⁴ Industrial Research Institute of Prefabricated Buildings and Energy-Saving Materials

* Correspondence: D202510014@xs.ustb.edu.cn

Abstract

Gravelly soil is widely distributed in the central and western regions of China and serves as a crucial fill material for transportation infrastructure. However, its poor gradation, poor water stability, and low freeze - thaw resistance limit its direct application. To address the problems of high energy consumption and high carbon emissions of existing solidifying agents (such as cement, lime) and achieve the resource utilization of waste foam concrete, this study took waste foam concrete as the raw material, prepared a novel gravel soil stabilizer through crushing, ball milling, and high - temperature calcination, and systematically studied the solidification performance (unconfined compressive strength, water stability, freeze - thaw resistance) of the prepared stabilizer on gravelly soil and its solidification mechanism. The results show that the prepared stabilizer can significantly improve the mechanical properties of gravelly soil. At a dosage of 30%, the unconfined compressive strength reached 6.5 MPa after 28 days, an increase of 333% compared to the control group. The water stability is enhanced with the increase of dosage, and the water stability coefficient is significantly improved at a dosage of 30%. In terms of freeze - thaw resistance, at a dosage of 30%, the mass loss rate was only 2% after 5 freeze - thaw cycles, and the unconfined compressive strength reached 9.56 MPa, an increase of 437% compared to the control group. XRD and SEM analysis indicate that the stabilizer generates cementitious products such as calcium silicate hydrate gel and katoite through hydration reactions, which fill the pores of gravelly soil, cement particles, and optimize the microstructure, thereby improving its mechanical properties, water stability, and freeze - thaw resistance. This study provides a new way for the efficient resource utilization of waste foam concrete and also offers a low - energy and environmentally friendly novel stabilizer for the reinforcement of gravel soil subgrades in cold regions.

Keywords: waste foam concrete; gravelly soil; soil stabilizer; freeze-thaw resistance

1. Introduction

Gravelly soil is abundant in the central and western regions of China and serves as a crucial fill material for transportation infrastructure. However, its inherent defects, such as the scarcity of fine particles and poor gradation, result in compaction difficulties, low unconfined compressive strength, and inadequate frost resistance [1,2]. Consequently, its direct application poses significant engineering risks. Particularly in the cold regions of western China, frequent freeze-thaw cycles exacerbate particle breakage, skeleton restructuring, and strength degradation, seriously compromising the safe operation of roads. Therefore, conducting research on the solidification of

gravelly soil to thoroughly elucidate its mechanical response mechanism and frost resistance characteristics under freeze-thaw conditions is key to enhancing the long-term performance of subgrade engineering in cold regions.

The solidifying agents commonly used for gravelly soil include cement [3], lime [4], cement-lime composite materials [5], and polymer materials [6]. As the most widely used solidifying material, cement possesses the advantages of high early strength, mature technology, and relatively low cost [7,8]. However, it suffers from defects such as high hydration heat, susceptibility to shrinkage cracking, and insufficient freeze-thaw durability [9–11]. Moreover, its production process requires high-temperature calcination, leading to environmental issues like high energy consumption and large carbon emissions. Although lime can significantly improve soil cohesion and plasticity, its strength growth is slow, and its early strength is low. Its solidification effect on coarse-grained soils like sandy gravel is limited by the fine particle content, and it similarly faces problems of high energy consumption, high pollution, and high carbon emissions caused by high-temperature calcination [12]. Cement-lime composite stabilizers, through complementary advantages, balance the early strength of cement with the long-term strength growth and crack resistance of lime, achieving a trade-off between economic efficiency and engineering performance. Nevertheless, they still face issues such as complex mix design and poor corrosion resistance. Polymer materials (such as epoxy resin), while capable of endowing solidified soil with extremely high strength, toughness, and excellent impermeability and corrosion resistance, are currently mainly limited to special engineering applications due to high costs, complex construction processes, and potential aging risks, making large-scale promotion in conventional subgrades difficult [13]. Therefore, the development of new solidifying agents that are low-cost, highly effective, low-carbon, and environment-friendly holds significant engineering value.

Foam concrete, as a new type of lightweight porous building material, have been widely used in wall insulation projects for buildings in the cold regions of Northwest China due to their excellent properties such as lightweight, sound absorption, and thermal insulation [14–16]. However, a large amount of waste foam concrete is generated due to new building construction, demolition of old buildings, and natural deterioration. Waste foam concrete is mainly composed of cement hydration products such as calcium silicate hydrate (C-S-H) gel, calcium hydroxide (CH), and ettringite (AFt), as well as unhydrated cement particles and numerous pore structures [17,18]. It is characterized by high porosity, low density, high water absorption, and relatively low mechanical strength. If improperly disposed, it not only occupies a large amount of land resources, but the fine dust generated during crushing also pollutes the atmosphere, and the alkaline leachate can easily lead to soil alkalization and groundwater contamination, posing serious harm to the ecological environment.

The treatment and disposal of waste foam concrete primarily rely on landfilling or stockpiling [19]. However, due to its low density and large volume, simple landfilling or stockpiling occupies a significant amount of land resources and contributes to the phenomenon of “garbage siege.” Furthermore, the abundant internal pores of foam concrete tend to form localized water retention layers within landfills, thereby affecting the stability of geological structures. Moreover, residual alkaline substances (such as calcium hydroxide) migrate with the leachate, causing alkaline contamination of the surrounding soil and water bodies [20,21]. Consequently, landfilling or stockpiling not only results in the waste of potential mineral resources but also causes environmental pollution.

In addition to landfilling, an increasing number of studies have focused on utilizing waste foam concrete to prepare recycled lightweight aggregates, lightweight insulation boards, and mortars. For instance, waste foam concrete is crushed and screened into artificial lightweight aggregates of different particle sizes for use in producing foamed cement self-insulation boards, geopolymer lightweight concrete, or as a substitute for lightweight aggregates [22,23]. It can also be processed into recycled foam concrete powder and recycled fine aggregate to replace cement and river sand, respectively, or combined with microencapsulated phase change materials to prepare multifunctional mortar [24,25]. However, due to the loose and porous original structure of waste

foam concrete, substantial amounts of fine powder are easily generated during the crushing process, leading to increased screening difficulty and energy consumption during the preparation of recycled aggregates. To meet aggregate gradation requirements, complex particle shaping and dust removal processes are often necessary, which significantly raises processing costs. Furthermore, the resulting recycled products, such as boards and mortars, typically exhibit low strength and high-water absorption, limiting their application to low-strength non-structural elements and hindering large-scale utilization [26,27]. Therefore, exploring a new resource utilization pathway that features simple technology, low cost, and superior product performance is of great significance for realizing the large-scale utilization of waste foam concrete.

In this study, a novel gravel soil stabilizer was prepared from waste foam concrete through processes of crushing, ball milling, and high-temperature calcination activation. The engineering performance of the stabilizer was systematically evaluated by testing the unconfined compressive strength, water stability, and freeze-thaw resistance of the stabilized gravel soil, and the solidification and strengthening mechanism was deeply revealed. This study not only offers a new avenue for the efficient resource utilization of waste foam concrete but also provides a low-cost and environmentally friendly novel stabilizer for gravel soil reinforcement.

2. Materials and Methods

2.1. Raw Materials

In accordance with the sampling methods specified in the Technical Specifications for Sampling and Sample Preparation of Industrial Solid Waste (HJ/T 20-1998), representative samples of waste foam concrete were selected from a construction waste dumping site, as shown in Fig.1. The obtained waste foam concrete was crushed into particles with a diameter of less than 5 mm using a small jaw crusher, and then ground in a ball mill for 30 min to obtain waste foam concrete powder with a particle size of < 0.075 mm. The regenerated powder was placed in a high-temperature box-type resistance furnace, calcined at 800 °C for 20 min [28,29], and then cooled to room temperature inside the furnace to prepare the gravel soil stabilizer. The prepared soil stabilizer is abundant in reactive C2S, CaO, and $C_{12}A_7$, attributed to the thermal decomposition of cement hydration products such as calcium silicate hydrate (C-S-H) gel, calcium hydroxide (CH), and ettringite (AFt) [30–32].



Figure 1. Waste foam concrete blocks obtained from construction waste dumping site.

The gravelly soil used in the experiment was taken from the Moli area of Lijie North Mountain and Guoye in Zhouqu County, Gansu, China. The slope has disordered joints and severe weathering, and the gravelly soil develops within the landslide zone. After field sampling, the soil samples were

sieved through a 5 mm square-hole sieve and then it were sealed with plastic wrap. The mineral composition of the gravelly soil was tested using an X - ray diffractometer, and the results are shown in Fig. 2. As can be seen from the figure, the mineral composition of the gravelly soil used in the experiment mainly consists of silica, limestone, and chlorite. According to the Standard for Soil Test Method GB/T 50123 - 2019, the basic physical properties of the gravelly soil were tested, and the results are shown in Table 1. From the data in the tables, it can be seen that the gravelly soil exhibited a natural moisture content of 11.5 %, which is close to its optimum moisture content of 10.6%, indicating favorable moisture conditions for compaction. Its maximum dry density was $2.22 \text{ g}\cdot\text{cm}^{-3}$, reflecting moderate compaction potential under optimal moisture. The particle gradation of the gravelly soil was analyzed by sieve analysis, and its particle gradation is shown in Table 2. The particle size distribution of the gravelly soil spanned a wide range of 0.25–40 mm. The highest particle content was found in the (2, 5) mm range (28.2 %), followed by (5, 10) mm (22.0 %) and (10, 20) mm (16.3 %).

Table 1. Basic physical parameters of gravelly soil.

Natural moisture content (%)	Maximum dry density ($\text{g}\cdot\text{cm}^{-3}$)	Optimum moisture content (%)	Coefficient of uniformity (C_u)	Coefficient of curvature (C_c)
11.5	2.22	10.6	8.37	1.21

Table 2. Particle gradation of gravelly soil.

Particle size range (mm)	(0.25,0.5)	(0.5,10)	(1,2)	(2,5)	(5,10)	(10,20)	(20,40)
Particle content (%)	1.2	13.8	8.5	28.2	22.0	16.3	10.0

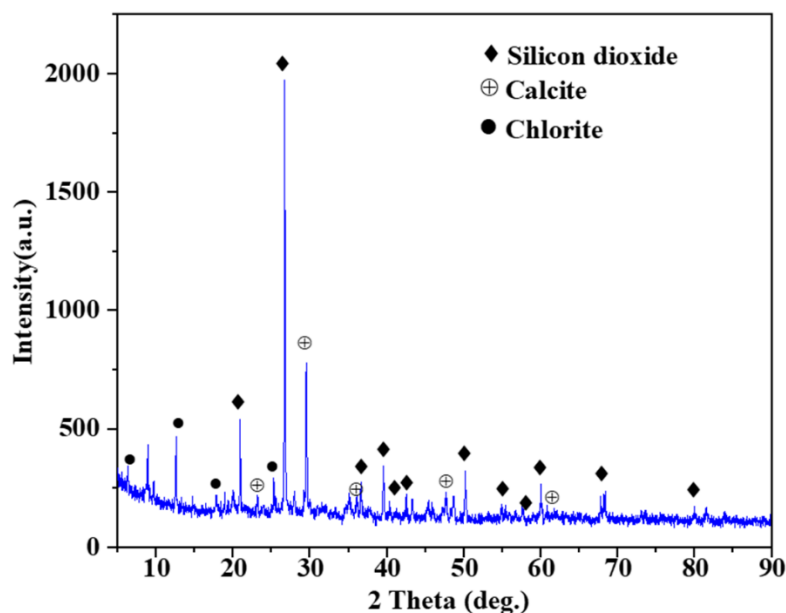


Figure 2. The XRD pattern of the gravelly soil.

2.2. Methods

2.2.1. Mix Proportion Design, Molding, and Curing of Stabilized Soil

The gravelly soil for the experiment and the prepared stabilizer were placed in a 105 °C oven and dried to constant weight. Based on the mass of the gravelly soil, the stabilizer was mixed with the gravelly soil in an external addition manner, with its dosages set to 0 % (control group), 10 %, 20 %, and 30 %, and they were named SGS0, SGS10, SGS20, and SGS30, respectively. The maximum dry density and optimum moisture content of the SGS0 and the stabilized soil with different stabilizer dosages were determined through compaction tests. Compaction molding of the untreated soil and stabilized soil was then conducted at their respective maximum dry density and optimum moisture content to ensure the compaction quality of the soil samples. The molding and curing process of stabilized soils are as follows:

Separately take 20 kg of untreated soil and stabilized soil with different stabilizer dosages, and divide each type of soil sample into 5–6 portions. Add a certain amount of test water to each soil sample, and the moisture content difference between adjacent samples is within 2 %. After fully mixing, seal them in self-sealing bags. The untreated soil needs to be left standing for 24 h for later use, while the stabilized soil must complete the compaction test within 1 h after the stabilizer is added. Conduct the compaction test according to the procedures in the Standard for Soil Test Method GB/T 50123 - 2019. After compaction, use a demolding device to remove the specimen from the compaction mold, take the soil from the center of the specimen, measure the moisture content in two groups, take the average value, and weigh it to the precision of 0.01 g. The calculation methods for moisture content and dry density are as follows:

$$\rho_d = \frac{\rho}{1 + 0.01\omega} \quad (2 - 5)$$

Where, ρ_d represents the dry density of the samples (g/cm^3); ρ denotes the wet density of the samples (g/cm^3).

Taking dry density and moisture content as the ordinate and abscissa, respectively, a relationship curve between dry density and moisture content can be plotted. The peak point on the curve represents the maximum dry density and optimum moisture content. The optimum moisture content and maximum dry density of gravelly soil under different stabilizer dosages are shown in Table 3.

Table 3. Mix proportion design of experimental stabilized soil.

Samples	dosage of stabilizer (%)	Maximum dry density (g/cm^3)	Optimum moisture content (%)
SGS0	0	2.22	10.60
SGS10	10	1.98	10.01
SGS20	20	1.80	10.32
SGS30	30	1.83	10.77

The test mold used in this study was a cylindrical steel mold, and the prepared specimens were cylindrical with both a diameter and height of 50 mm, as shown in Fig.3. During sample preparation, the stabilized soil mixture was weighed, mixed, and filled into the mold according to the mix proportions shown in Table 3. After filling, the entire mold assembly was placed on a compression machine and loaded at a rate of 1 mm/min, with a static pressure holding time of 2 min. After releasing the pressure, the mold was removed and placed on an electric demolding machine to eject the specimen. The mass of the specimen was weighed to the nearest 0.01 g, and the height and diameter were measured using a vernier caliper to the nearest 0.1 mm. The appearance was inspected, and specimens that did not meet the requirements for height and mass were discarded. Immediately after weighing, the specimens were wrapped in plastic film, labeled, covered with damp towels, and transferred to a standard curing box for curing under conditions of 20 ± 2 °C and relative humidity ≥ 95

%. Three parallel specimens were prepared for each curing age. Upon reaching the corresponding curing ages, the specimens were taken out for unconfined compressive strength tests, water stability tests, and freeze-thaw cycle tests.

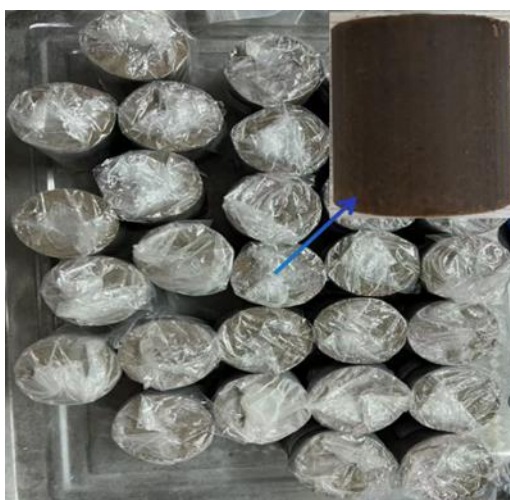


Figure 3. Stabilized soil specimens prepared for testing.

2.2.2. Unconfined Compressive Strength (UCS) Test

The stabilized soil specimens cured to the specified age were taken out, and the unconfined compressive strength test was conducted in accordance with the Standard for Soil Test Method (GB/T 50123-2019). The test adopted a strain-controlled mode with a loading rate set at 1 mm/min. The termination criteria were as follows: when the axial pressure reached a peak or stable value, loading continued until the axial strain increased by 3% before stopping the test. If the axial pressure did not exhibit a peak or stable value, the test was terminated when the axial strain reached 20%. The calculation methods for unconfined compressive strength, axial stress, and axial strain are as follows:

$$\varepsilon = \frac{\Delta h}{h_0} \times 100 \quad (2-6)$$

$$A_0 = \frac{1}{4} \pi D^2 \quad (2-7)$$

$$A_a = \frac{A_0}{1 - 0.01\varepsilon} \quad (2-8)$$

$$\sigma = \frac{P}{A_a} = \frac{P \times (1 - 0.01\varepsilon)}{A_0} \quad (2-9)$$

Where, ε represents axial strain (%); Δh denotes the height reduction of the specimen due to compression (mm); h_0 represents initial height of the specimen before compression (mm); A_0 denotes initial cross-sectional area of the specimen (mm^2); D represents diameter of the specimen (mm); A_a denotes corrected cross-sectional area of the specimen (mm^2); P represents axial force (N); σ denotes axial stress (MPa).

2.2.3. Water Stability Test

Two methods were adopted to evaluate the water stability of the stabilized soil. The first method evaluates the stability of the stabilized soil in water based on the degree of reduction in the unconfined compressive strength of the specimens before and after immersion. In the experiment,

specimens cured to the age of 7 days under standard conditions were immersed in water. The disintegration status was observed for immersion periods ranging from 1 to 7 days. Unconfined compressive strength tests were then conducted on specimens with different immersion times to evaluate water stability through strength loss. The second method refers to the Standard Soil Stabilizing Admixtures (CJ/T 486-2015). The water stability coefficient of the stabilized soil is obtained by calculating the ratio of the unconfined compressive strength of specimens subjected to 1 day of immersion curing after standard curing for 6, 27, and 89 days to the unconfined compressive strength of specimens under standard curing for 7, 28, and 90 days. The calculation method for the water stability coefficient is as follows:

$$\gamma_s = \frac{UCS_{water}}{UCS} \times 100 \quad (2 - 11)$$

Where, γ_s represents water stability coefficient (%); UCS_{water} represents compressive strength of the specimen immersed for the last day within the curing period (MPa); UCS represents unconfined compressive strength of the specimen without immersion during the curing period (MPa).

2.2.4. Freeze-Thaw Cycle Test

Freeze-thaw cycle tests were conducted on stabilized soil specimens with different mix proportions after standard curing for 28 days. The number of freeze-thaw cycles was set at 0, 1, 3, and 5. The freezing temperature was set at $-20\text{ }^\circ\text{C}$, and the melting temperature was set at $20\text{ }^\circ\text{C}$. The cooling and heating rates of the test chamber were $5\text{ }^\circ\text{C/h}$. The initial temperature of the freezing process was $20\text{ }^\circ\text{C}$. The test chamber cooled down to $-20\text{ }^\circ\text{C}$ at a rate of $5\text{ }^\circ\text{C/h}$, taking a total of 8 hours, and then maintained at $-20\text{ }^\circ\text{C}$ for 4 hours; thus, the total freezing time was 12 hours. Subsequently, the temperature was raised to $20\text{ }^\circ\text{C}$ at a rate of $5\text{ }^\circ\text{C/h}$, which took 8 hours, followed by maintaining at $20\text{ }^\circ\text{C}$ for 4 hours for melting; thus, the melting time was also 12 hours. The duration of one freeze-thaw cycle was 24 hours, ensuring complete freezing and melting of the specimens. Finally, the freeze-thaw resistance of the stabilized soil was characterized based on the changes in mass and unconfined compressive strength before and after freeze-thaw. The formula for calculating the mass change rate is as follows:

$$W_n = \frac{m_0 - m_n}{m_0} \quad (2 - 12)$$

Where, W_n represents mass change rate of the stabilized soil specimen (%); m_0 represents the mass of the stabilized soil specimen before the freeze-thaw cycle test (g); m_n represents mass of the stabilized soil specimen after the n -th freeze-thaw cycle (g).

2.2.5. Material Analytical Methods

A Bruker D8 Advance X-ray powder diffractometer (XRD) was employed to determine the phase composition of the samples, utilizing $\text{Cu K}\alpha_{1,2}$ radiation at 50 kV and 45 mA. The scanning range was set between 5° and 90° (2θ) with a continuous scan rate of $5^\circ/\text{min}$. For sample preparation, the central portion of the crushed stabilized soil was isolated and immersed in anhydrous ethanol for 48 hours, followed by oven drying. Subsequently, the dried material was pulverized and passed through a $45\text{ }\mu\text{m}$ square-hole sieve before analysis. The microscopic morphology of the samples was examined using a scanning electron microscope (SEM, Hitachi S4800, Japan). Prior to observation, the powder samples were mounted on a sample holder using conductive adhesive and subjected to gold sputter-coating to improve their electrical conductivity. Once the coating process was completed, the samples were transferred into the microscope for imaging and analysis.

3. Results and Discuss

3.1. The Effect of Soil Stabilizer on the Mechanical Properties of Stabilized Gravelly Soil

Figure 4 illustrates the variation trend of unconfined compressive strength (UCS) of stabilized soil at different curing ages (1d, 7d, 28d, and 96d) under various stabilizer dosages. The unconfined compressive strength values of the gravelly soil without soil stabilizer at 1d, 7d, 28d, and 96d are 1.0 MPa, 1.2 MPa, 1.5 MPa, and 1.3 MPa, respectively, indicating that the UCS of the gravelly soil without soil stabilizer does not increase with the extension of curing age. When different amounts of soil stabilizer are added, it can be observed that with the increase of soil stabilizer dosage, the UCS of stabilized soil at all curing ages shows a significant upward trend. At the same dosage, the UCS enhances with the extension of curing age, with the 96d age showing the highest strength, followed by 28d, 7d, and 1d. When the soil stabilizer dosage increases to 30%, the UCS values at each curing age reach approximately 4.5 MPa, 5.5 MPa, 6.5 MPa, and 9.5 MPa, respectively, representing strength increase amplitudes of about 350 % (1d), 358 % (7d), 333 % (28d), and 631 % (96d) compared to the control group. Moreover, in the low dosage range (0~10%), the growth of UCS is relatively gentle, while in the high dosage range (20~30 %), the growth amplitude increases significantly, especially for the 96d age, indicating that the effect of soil stabilizer dosage on long-term strength is more prominent.

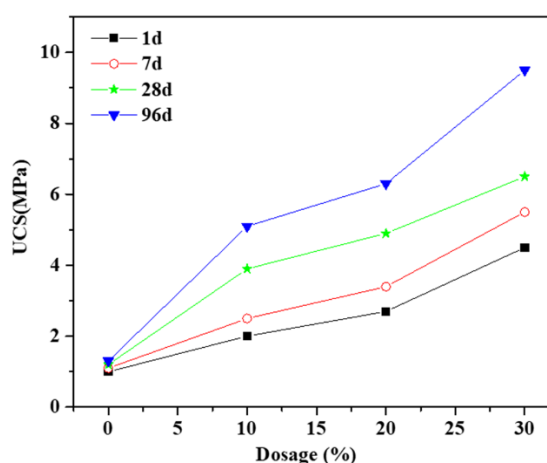


Figure 4. The effect of stabilizer dosage on the unconfined compressive strength of gravelly soil at different curing ages.

Figure 5 illustrates the effect of stabilizer dosage on the σ - ϵ curves of gravelly soil. It can be observed from the figure that the variation trends of σ - ϵ curves for gravelly soil are basically the same under different curing ages and stabilizer dosages. The σ - ϵ curves of stabilized gravelly soil can be divided into four stages: (1) compaction stage, (2) elastic deformation stage, (3) plastic deformation stage, and (4) stress drop stage. This is mainly because, at the initial loading stage, the compressive stress is relatively small, and the gravelly soil particles undergo relative sliding and rearrangement under pressure, resulting in a decrease in pore volume and thus forming the compaction stage. All gravelly soil samples exhibit significant plastic deformation during this stage. As the compaction stage is completed, a continuous and dense rigid skeleton is formed between the gravelly soil particles inside the sample, thus exhibiting obvious linear elastic deformation behavior. However, as the compressive stress continues to increase, microcracks continuously generate inside the sample, and the slip between particles increases, leading to an increase in plastic deformation. When the compressive stress reaches the bearing limit of the stabilized soil, the internal cracks in the sample coalesce and structural failure occurs, causing a rapid drop in stress, which is manifested as the stress drop stage in the σ - ϵ curves.

In the compaction stage (Stage 1), when the stabilizer dosage is the same, the plastic deformation amount of the gravelly soil samples in this stage shows a decreasing trend with the increase of curing age. For example, when the stabilizer dosage is fixed at 20%, the plastic deformation amount of the gravelly soil is about 3.5% at 1 d of curing, while it decreases to 2.4%, 1.5%, and 1.3% when cured for 7 d, 28 d, and 90 d, respectively. This indicates that the addition of stabilizer can significantly reduce the plastic deformation amount in the compaction stage, thereby improving the volume stability of the gravelly soil. When the stabilizer dosage in the gravelly soil is changed, the plastic deformation amount of the gravelly soil usually increases with the increase of stabilizer dosage in the early curing ages, as shown in Fig. 5(a, b, c). This is mainly because the stabilizer prepared from foamed concrete has not been fully hydrated in the early curing ages, resulting in weak gelling performance for the gravelly soil, and its own high porosity leads to a higher volume compression rate during compression. However, when the curing age is extended to 90 d, the plastic deformation amount of the gravelly soil shows a decreasing trend with the increase of stabilizer dosage, as shown in Fig. 5(d). This is mainly because with the increase of curing age, the stabilizer undergoes continuous reaction, and its cementation effect on the gravelly soil particles continuously increases, thereby reducing the plastic deformation amount of the gravelly soil and improving its volume stability.

In the elastic deformation stage (Stage 2), under the same stabilizer dosage, the elastic modulus of gravelly soil shows a significant increasing trend with the extension of curing age (as shown in Fig. 6). When the dosage is 10%, the elastic modulus of the stabilized gravelly soil specimen is 1294.8 kPa at 1 day of curing, increases to 1647.4 kPa at 7 days, and further rises to 2537.3 kPa at 28 days. When the dosage is 20%, the elastic modulus of the stabilized gravelly soil at 1d, 7d, and 28d of curing is 1667.9 kPa, 2358.0 kPa, and 3605.7 kPa, respectively. This indicates that the longer the curing age, the more sufficient the hydration of the stabilizer, and the more hydration products with cementitious properties can be produced, which strengthens the cementation effect between gravelly soil particles, thus continuously increasing the elastic modulus of the stabilized body. At the same curing age, the elastic modulus increases significantly with the increase of stabilizer dosage. At 28 days of curing, the elastic modulus of the sample with 30% dosage is 4077.0 kPa, which is significantly higher than that of the 20% dosage (3605.7 kPa) and 10% dosage (2537.3 kPa), being approximately 14% and 64% higher, respectively; at 7 days of curing, the elastic modulus of the 30% dosage sample is 2971.5 kPa, about 26% higher than that of the 20% dosage (2358.0 kPa) and about 80% higher than that of the 10% dosage (1647.4 kPa); at 1 day of curing, the elastic modulus of the 30% dosage sample is 2772.6 kPa, significantly higher than that of the 20% dosage (1667.9 kPa) and 10% dosage (1294.8 kPa), being approximately 66% and 114% higher, respectively. The higher the stabilizer dosage, the more total products generated by the hydration reaction, and the stronger the cementation effect on the particles. At high dosages (such as 30%), more hydration products not only fill the original pores but also form a stronger skeleton structure, effectively inhibiting the relative sliding of particles, so the elastic modulus is significantly higher than that of low-dosage samples (such as 10% and 20%).

In the plastic deformation stage (Stage 3), the curve of low - dosage samples (e.g., 10%) is relatively flat, and the plastic deformation is larger. In contrast, the plastic deformation stage of high - dosage samples (e.g., 30%) is significantly shortened. This indicates that at high dosages, the cementation structure is denser, particle sliding and microcrack propagation are inhibited, and the material brittleness increases. Figure 5(a) shows that for the 10% dosage sample at 1d curing age, the strain range of the plastic deformation stage is about 1.0% - 3.0%, while for the 30% dosage sample, it is only about 0.5% - 2.0%. In the stress drop stage (Stage 4), the stress drop rate of high - dosage samples is slower, and the descending segment of the curve is more gradual. For example, the slope of the stress drop segment of the 30% dosage sample at 28d curing age is only 60 % of that of the 10 % dosage sample, reflecting that the failure process is slower and the toughness of the cementation structure is better under high dosage.

Overall, the soil stabilizer significantly changes the σ - ε curves of gravelly soil by affecting the mechanical behaviors in each stage: high dosage enhances the stiffness in the initial compaction and

elastic stages, inhibits plastic deformation, delays the failure process, and increases the unconfined compressive strength.

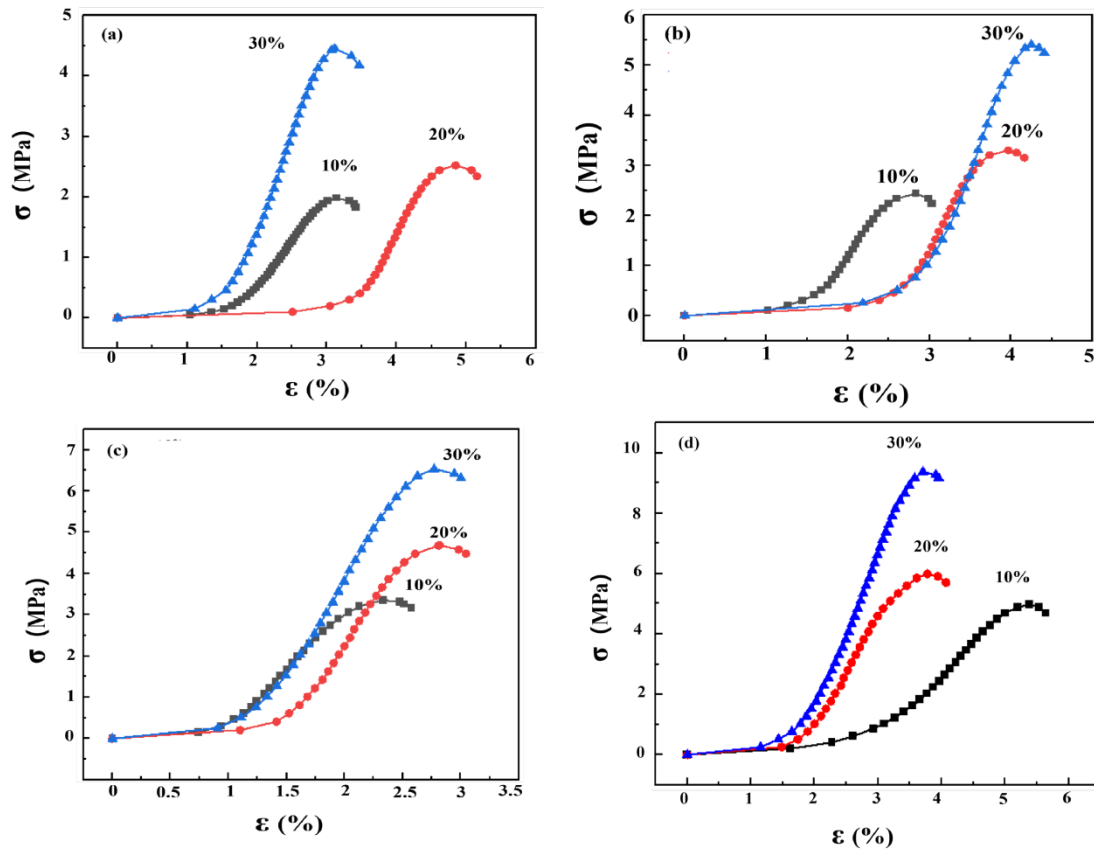


Figure 5. The effect of soil stabilizer dosage on the mechanical and deformation properties of gravelly soil during uniaxial compression failure process at different standard curing ages (a) 1 d; (b) 7 d; (c) 28 d; (d) 90 d.

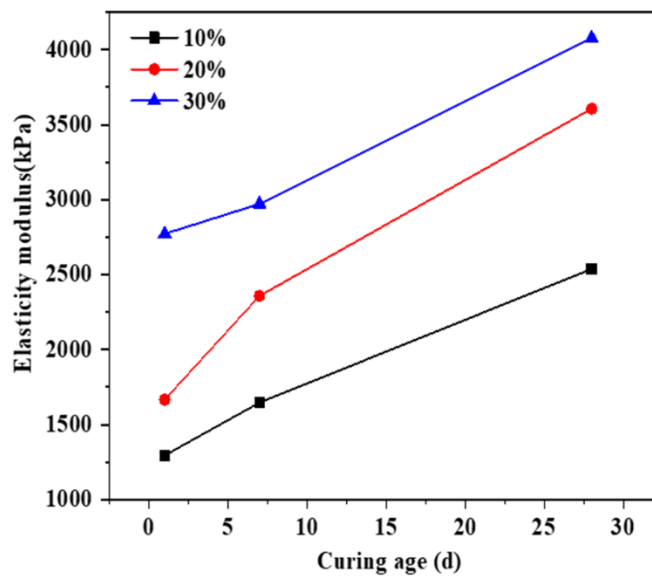


Figure 6. The effect of soil stabilizer dosage on the elasticity modulus of stabilized gravelly soil cured at different ages.

Table 2. S, CaO, and $C_{12}A_7$) that hydrate to form substantial amounts of calcium silicate (alumina) hydrate (C-S(A)-H) gel, which acts as the primary binder coating soil particles and bridging inter-particle voids. This results in a denser cementation structure and higher strength [33–35]. Over the long term, the strength gain is further sustained by the pozzolanic reaction. The reactive CaO contained in soil stabilizer can react with silica in the gravelly soil, generating secondary C-S-H gel. These secondary products progressively fill the capillary pores and micro-voids within the soil matrix, leading to a significant reduction in porosity and a denser microstructure [36–38]. Consequently, the mechanical properties continue to improve significantly under long-term curing conditions.

3.2. The Effect of Soil Stabilizer on the Water Stability of Stabilized Gravelly Soil

As shown in Fig.7 (a), specimens prepared with gravelly soil without stabilizer or with only 10% stabilizer cannot remain stable when completely immersed in water; they disintegrate and lose their mechanical strength. When the stabilizer dosage reaches 20% and 30%, the stabilized gravelly soil samples can maintain stability when completely immersed in water, as shown in Fig.7 (b). Meanwhile, as shown in Table 4, after 7 days of complete immersion, the specimens prepared with stabilized gravelly soils with 20 % and 30 % stabilizer maintained their integrity, indicating that when the stabilizer dosage exceeds 20%, the addition of stabilizer can effectively improve the water stability of gravelly soil.

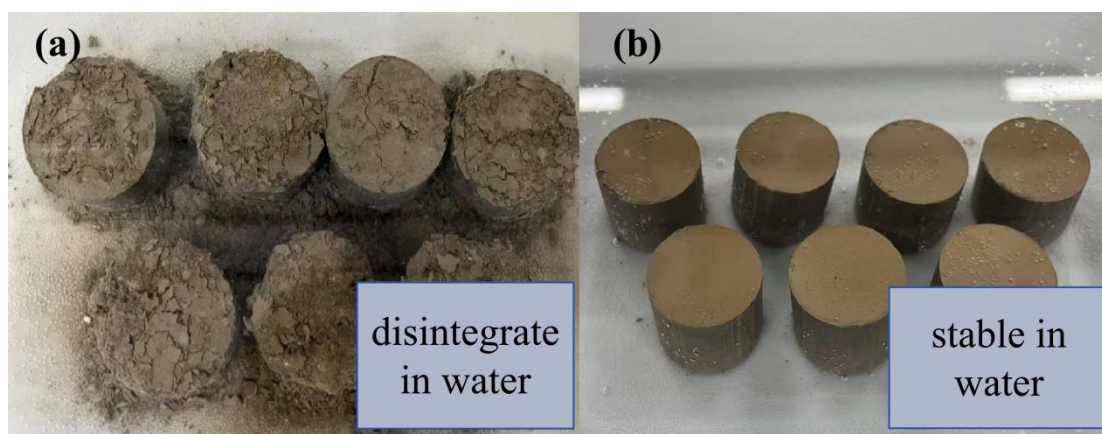


Figure 7. Typical appearance of different stabilized gravelly soils after water exposure: (a) disintegrate in water; (b) remain stable in water.

Table 4. Effect of stabilizer dosage on the water stability of stabilized gravelly soil .

dosage of soil stabilizer (%)	soaking time (d)						
	1d	2d	3d	4d	5d	6d	7d
0	disintegrate	—	—	—	—	—	—
10	disintegrate	—	—	—	—	—	—
20	stable	stable	stable	stable	stable	stable	stable
30	stable	stable	stable	stable	stable	stable	stable

The variation of UCS at different soaking times was tested for the specimens with 20% and 30% stabilizer dosages, the results are shown in Fig.8. Overall, as soaking time increases, the UCS of both specimens reduces. However, the specimen with 30% stabilizer exhibits better water stability than that of the specimen with 20% stabilizer. Among the unsoaked specimens, the stabilized gravelly soil with 30% stabilizer has a higher initial UCS (5.41 MPa) than the one with 20 % stabilizer (3.31 MPa). When the specimens were soaked for 1 d, both specimens show a significant decrease in UCS. The specimen with 20 % stabilizer drops to ≈ 1.05 MPa, while specimen with the 30% stabilizer decreases

to 1.90 MPa. During the soaking period of 2–3 d, the UCS of the 20% stabilizer specimen fluctuates (rising to 1.90 MPa at 2 d, then dropping to 0.80 MPa at 3 d). In contrast, the UCS of the specimen with 30% stabilizer increases to a peak of 3.08 MPa at 3 d, indicating better strength recovery. For the soaking period of 4–7 d, the UCS of the specimen with 20% stabilizer remains relatively low (0.7–1.1 MPa) with minor fluctuations, whereas the UCS of the specimen with 30% stabilizer gradually decreases but stays consistently higher (1.3–1.9 MPa) than that of the specimen with 20% stabilizer throughout this period. In conclusion, the water stability of stabilized gravelly soil increases as the stabilizer dosage increases, and a significant improvement in water stability is observed when the stabilizer dosage reaches 30%.

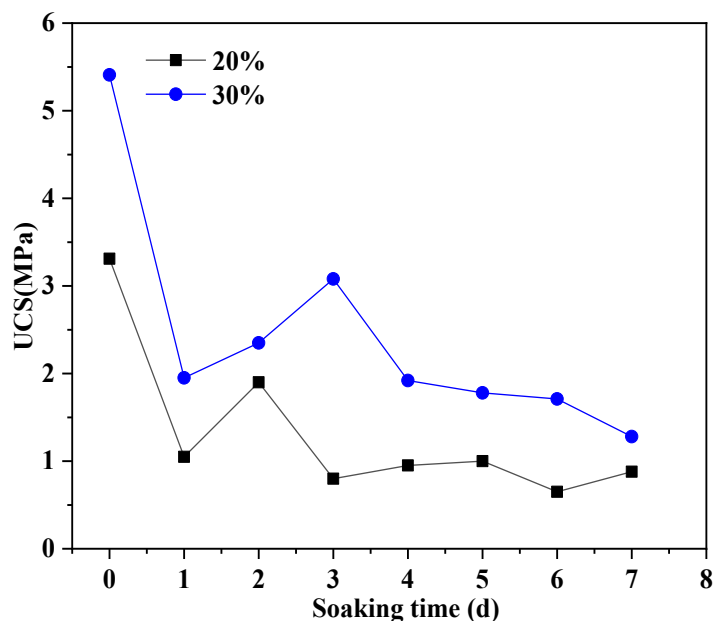


Figure 8. Effect of soaking time on the unconfined compressive strength of stabilized gravelly soil bodies with different stabilizer dosages.

Figure 9 shows the effect of curing age on the water stability of stabilized gravelly soil with different stabilizer dosages. As can be seen from the figure, when the stabilizer dosage is 10%, the water stability coefficients (γ_s) of stabilized gravelly soil at different curing ages are relatively low, and the γ_s does not increase significantly with the increase of curing age. When the stabilizer dosage is increased to 20%, the γ_s of stabilized gravelly soil at each curing age are significantly improved. Compared with the 10% dosage group, the increase in γ_s can reach 2–4 times (e.g., an increase of about 225% at 7 days and about 433% at 28 days). At the same time, it can be seen that when the curing age reaches 28 days, the γ_s reaches the maximum value, and continuing to increase the curing time to 90 d does not significantly improve the γ_s of stabilized gravelly soil. When the stabilizer dosage is further increased to 30%, the γ_s of stabilized gravelly soil at different curing ages continue to increase significantly. Compared with the 20% dosage group, the increase in γ_s is further expanded (e.g., an increase of about 162.5% at 28 days). Moreover, it can be observed that the γ_s of the stabilized soil reaches the maximum value at 28 days of curing, and subsequent increase in curing time cannot further increase the γ_s of the stabilized soil. This indicates that the stabilizer dosage is still the main influencing factor on the water stability of stabilized gravelly soil, and the appropriate curing age is generally 28 days. Continuing to increase the curing age will not improve the water stability of stabilized gravelly soil. This is mainly because with the increase of stabilizer dosage, the amount of stabilizer participating in the reaction per unit volume of soil increases, thus producing more cementitious hydration products. These hydration products can effectively fill the soil pores and form a stable structure. At the same time, the hydration reaction of the stabilizer is basically completed within 28 days. At this time, the hydration products have reached a saturated state, and continuing

to extend the curing time will not produce new hydration products, so the water stability of stabilized gravelly soil will not be further improved.

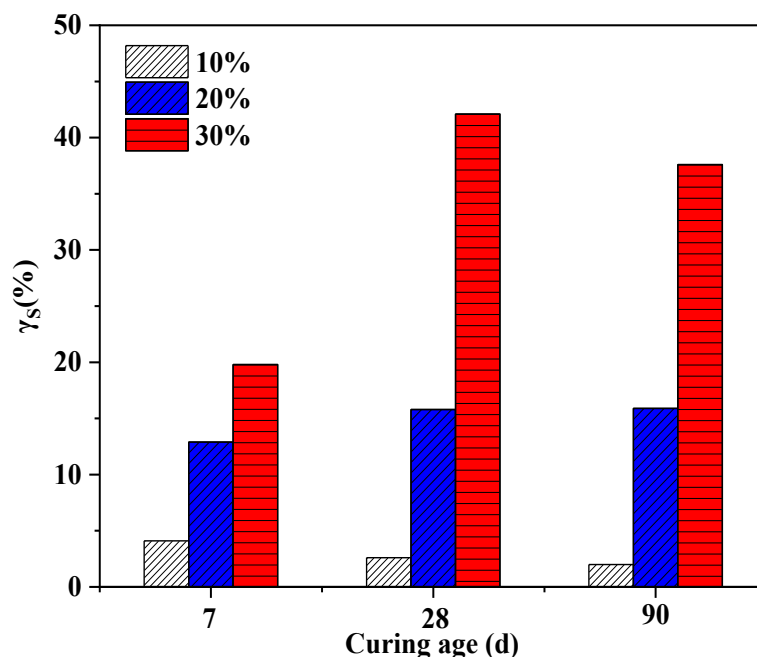


Figure 9. The effect of curing age on the water stability of stabilized gravelly soil with different stabilizer dosages.

3.3. The Effect of Soil Stabilizer on the Freeze - Thaw Resistance of Stabilized Gravelly Soil

Figure 10 shows the effect of stabilizer dosage on the mass loss rate of stabilized gravelly soil under different freeze - thaw cycles. As can be seen from the figure, the stabilizer dosage has a significant effect on the mass loss rate of stabilized gravelly soil during freeze - thaw cycles. First, as the stabilizer dosage increases from 0 % to 30%, the mass loss rate under each freeze - thaw cycle shows a clear downward trend. For example, when no stabilizer is added (0 % dosage), the mass loss rates after 1, 3, and 5 freeze - thaw cycles are approximately 2 %, 7 %, and 7 %, respectively. When the dosage is increased to 30 %, the corresponding mass loss rate decreases to approximately 0.5 %, 1 %, and 2 %, respectively, indicating that the stabilizer can effectively reduce the mass loss of the soil caused by freeze - thaw cycles. Second, under the same stabilizer dosage, the mass loss rate increases with the increase of freeze - thaw cycles (for example, when the dosage is 0 %, the mass loss rate after 5 cycles is significantly higher than that after 1 cycle), but the increase in the high - dosage group is smaller than that in the low - dosage group. For example, when the dosage is 30 %, the increase in mass loss rate after 5 cycles compared with 1 cycle is about 1.5 %, while when the dosage is 0%, the increase reaches 5 % points, indicating that a high - dosage stabilizer can weaken the aggravating effect of the increase in freeze - thaw cycles on mass loss. This is mainly because the stabilizer participates in the hydration reaction to generate cementitious products, which fill the soil pores and enhance structural stability, thereby reducing the damage to the soil caused by water migration and ice expansion during freeze - thaw. And finally, the mass loss rate decreases with the increase of dosage. This rule remains consistent under multiple freeze - thaw cycles, further verifying the effectiveness of the stabilizer in improving the freeze - thaw resistance of stabilized gravelly soil.

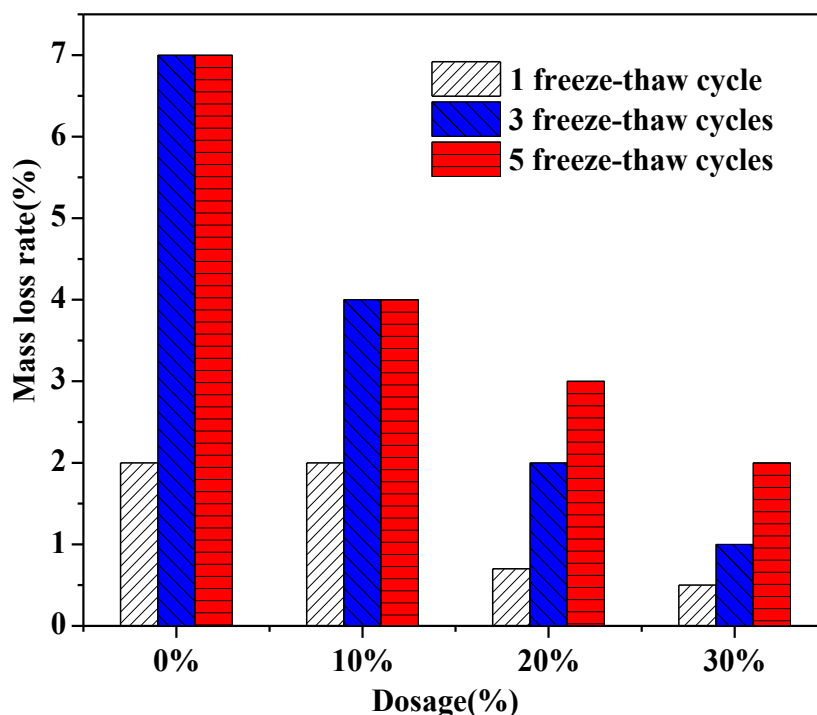


Figure 10. Effect of stabilizer dosage on the mass loss rate of stabilized gravelly soil under different freeze - thaw cycles.

Figure 11 shows the effect of stabilizer dosage and freeze - thaw cycles on the unconfined compressive strength (UCS) of stabilized gravelly soil. Compared with the gravelly soil without stabilizer, when the stabilizer dosage increases to 30 %, the UCS under each freeze - thaw cycle shows a significant increasing trend. For example, when no stabilizer is added (0 % dosage), the UCS after 1 freeze - thaw cycle is 0.99 MPa, while when the dosage is increased to 30%, the UCS after 1 cycle increases to 5.69 MPa, with an increase of 475%. After 3 cycles, the UCS at 0 % dosage is about 1.34 MPa, and it increases to 6.67 MPa at 30 % dosage, with an increase of about 398%. After 5 cycles, the UCS at 0 % dosage is 1.78 MPa, and it increases to 9.56 MPa at 30 % dosage with an increase of about 437%. This indicates that the stabilizer can effectively enhance the freeze - thaw resistance of stabilized gravelly soil, and the higher the dosage, the more significant the improvement in freeze - thaw resistance. Under the same stabilizer dosage, the UCS increases with the number of freeze - thaw cycles. At low dosages (0 % and 10 %), the UCS shows only a modest increase with more cycles—for instance, at 0 % dosage, it rises from 0.99 MPa (1 cycle) to 1.78 MPa (5 cycles), and at 10% dosage, from 3.19 MPa to 4.62 MPa over the same period. In contrast, at a high dosage of 30 %, the UCS exhibits a rapid upward trend, jumping from 5.69 MPa (1 cycle) to 9.56 MPa (5 cycles) as cycles increase.

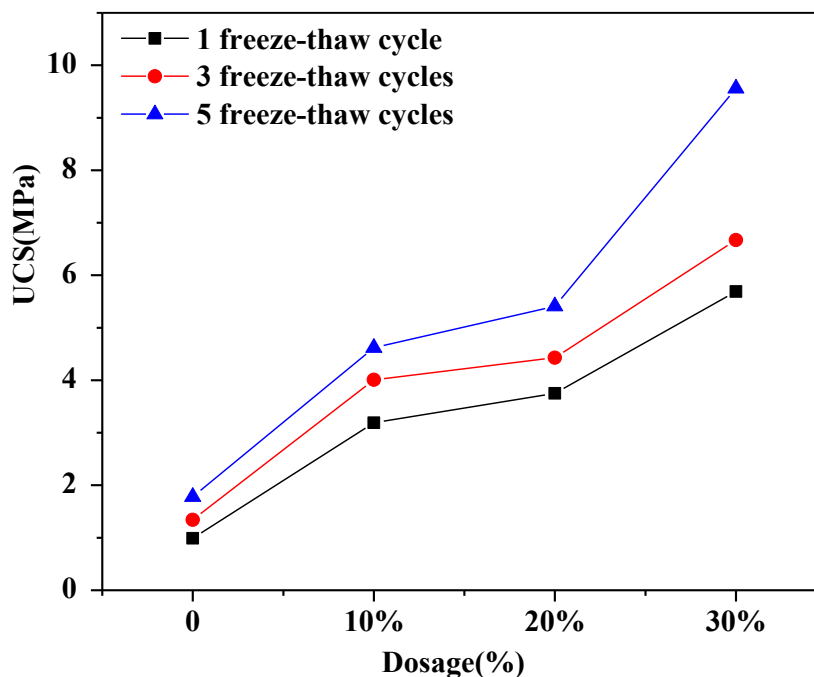


Figure 11. The effect of stabilizer dosage and freeze - thaw cycles on the unconfined compressive strength (UCS) of stabilized gravelly soil.

In summary, the stabilizer can significantly improve the freeze - thaw resistance of gravelly soil. The higher the stabilizer dosage, the higher the UCS of the stabilized gravelly soil after freeze - thaw cycles. However, the effect of the number of freeze - thaw cycles varies with different stabilizer dosages. When the stabilizer dosage is low, the increase in UCS of the stabilized gravelly soil due to freeze - thaw cycles is relatively small. However, when the stabilizer dosage increases, the number of freeze - thaw cycles can significantly enhance the UCS of the stabilized gravelly soil. This is mainly because the hydration reaction of the stabilizer depends on water and temperature. During freeze - thaw cycles, the repeated temperature changes can promote the uniform distribution of water in the soil^[39], enabling the incompletely reacted stabilizer particles to fully contact water and accelerating the generation of cementitious products^[40]. These cementitious products further fill the pores and cement the particles, enhancing the overall strength of the soil. Therefore, freeze - thaw cycles can improve the UCS of the stabilized soil to a certain extent, and this enhancing effect becomes more pronounced as the stabilizer dosage increases

3.4. Discuss on the Mechanism of the Soil Stabilizer on Gravelly Soil Stabilization

Figure12 shows the XRD patterns of the gravelly soil stabilized with different amount of soil stabilizer cured for 28 days. The main mineral phases in the gravelly soil without stabilizer are quartz, calcium carbonate, and chlorite. Firstly, it can be observed that with the increase of stabilizer dosage, the characteristic diffraction peaks of the quartz phase in the stabilized gravelly soil show a decreasing trend. This is mainly because the waste foamed concrete contains a large amount of calcium - containing compounds (such as calcium silicate hydrate gel, calcium hydroxide, calcium carbonate, etc.). These calcium - containing compounds are converted into highly active calcium oxide through high - temperature calcination at 800 °C and remain in the prepared stabilizer. When the stabilizer is added to the gravelly soil, under the action of water, the quartz in the gravelly soil will undergo a hydration reaction with the active calcium oxide in the stabilizer to form calcium silicate hydrate gel, which leads to the decrease in the intensity of the characteristic diffraction peaks of quartz in the gravelly soil. Secondly, when the stabilizer dosage in the gravelly soil reaches 30 %, katoite can be observed as a newly appeared phase in the stabilized soil. This is mainly because the waste foamed concrete contains a large amount of aluminum - containing hydration products

(ettringite), which can decompose into active alumina during high - temperature calcination and exist in the stabilizer. Under the presence of water, it can react again with the active calcium oxide in the stabilizer to form katoite. Fig.13 shows the SEM images of raw gravelly soil (a) and stabilized gravelly soil with 30% soil stabilizer (b). As can be seen from the figure, the raw gravelly soil, as shown in Fig.13 (a), exhibits a loose particle - packed structure with large inter - particle pores and no obvious cementing substances. In contrast, the stabilized gravelly soil with 30% stabilizer has particles tightly cemented by cementitious products, with pores effectively filled, forming a denser microstructure and tighter inter - particle connections, as shown in Fig.13 (b). This filling and improvement of the microstructure corresponds with the generation of cementitious products in XRD, together illustrating that the stabilizer optimizes the microstructure of gravelly soil by generating cementitious products, thereby enhancing its mechanical properties and freeze - thaw resistance.

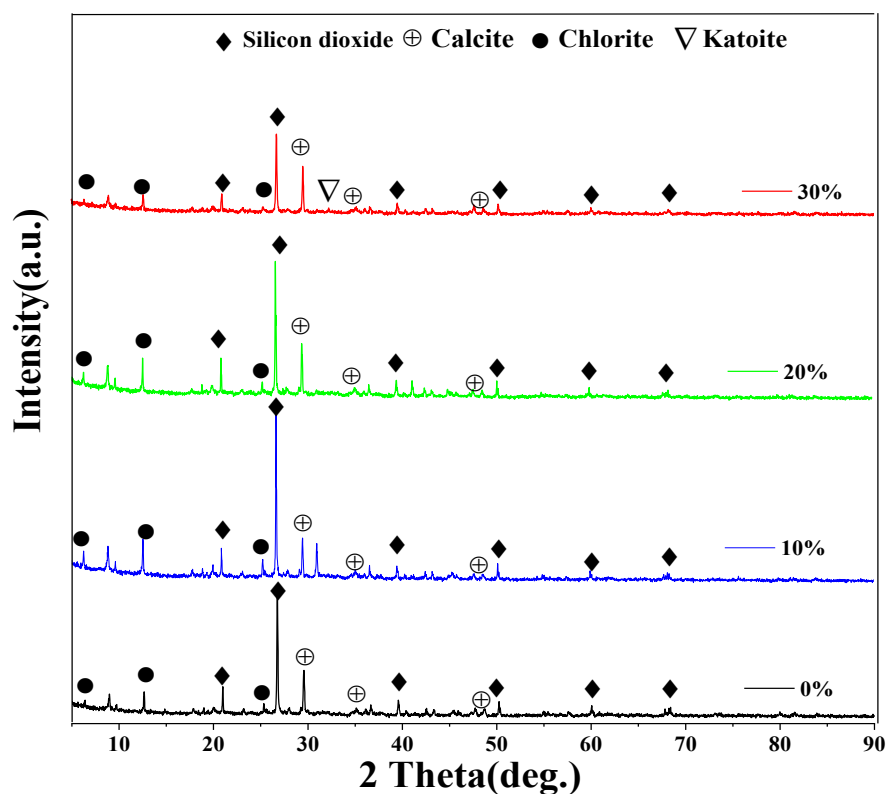


Figure 12. XRD patterns of the gravelly soil stabilized with different amount of soil stabilizer cured for 28 days.

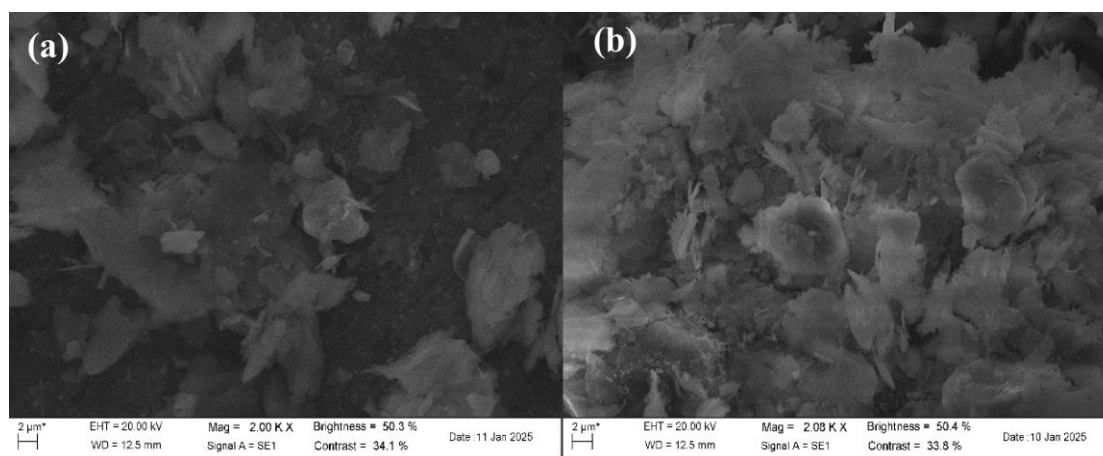


Figure 13. SEM images of (a) raw gravelly soil and (b) stabilized gravelly soil with 30 % soil stabilizer.

Figure 14 shows the XRD patterns of the stabilized soil with 30% stabilizer dosage before and after freeze - thaw cycles after 28 days of curing. As can be seen from the figure, the intensity of the characteristic diffraction peaks of the quartz phase in the gravelly soil further weakens after freeze - thaw, and the newly appeared tacharanite phase can be observed. This indicates that during the freeze - thaw process, the water in the stabilized gravelly soil repeatedly freezes, expands, melts, and diffuses, uniformly distributing the water in the soil pores. The incompletely reacted active calcium oxide in the stabilizer fully contacts with water and promotes its reaction with the quartz phase in the gravelly soil, ultimately accelerating the formation of cementitious calcium - silicate phases (tacharanite). The formed cementitious tacharanite can fill the pores of the gravelly soil, cement the particles, and form a denser microstructure.

In conclusion, it is precisely due to the formation of a large amount of these cementitious products, which fill the pores between the gravelly soil and better cement the particles in the gravelly soil, that the mechanical properties, water resistance, and freeze - thaw resistance of the soil are significantly enhanced.

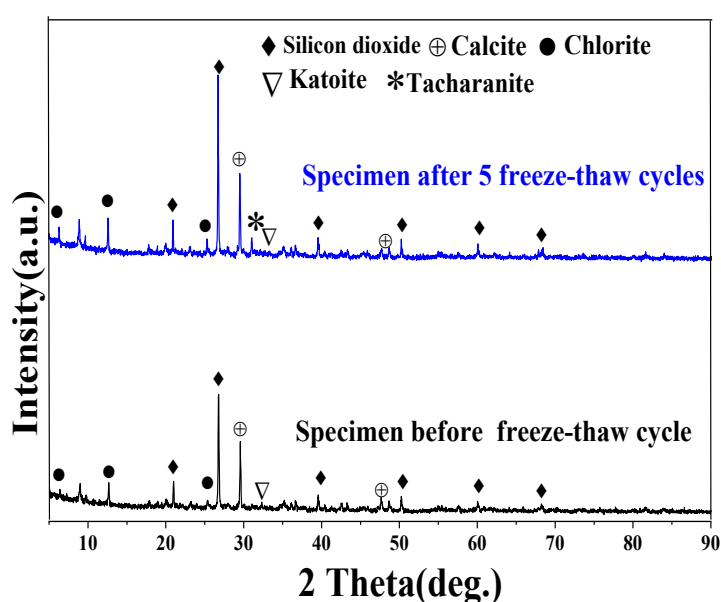


Figure 14. XRD patterns of stabilized gravelly soil before and after freeze-thaw cycles (cured for 28 days, with a soil dosage of 30%).

4. Conclusion

This study prepared a novel gravel soil stabilizer from waste foam concrete, which can effectively improve the mechanical properties, water stability, and freeze - thaw resistance of gravelly soil. The higher the dosage of the stabilizer, the higher the unconfined compressive strength, water stability coefficient, and post - freeze - thaw strength of the stabilized gravelly soil, and the lower the mass loss rate. The solidification mechanism lies in that the active calcium oxide in the stabilizer undergoes hydration reactions with minerals such as quartz in the gravelly soil to generate cementitious products like calcium silicate hydrate gel and katoite. These products fill pores, cement particles, and form a dense microstructure, thereby enhancing the overall performance of the soil mass. Freeze - thaw cycles promote the uniform distribution of water, accelerate the contact between the incompletely reacted stabilizer and water, and further generate cementitious products such as tacharanite, thus strengthening the soil's freeze - thaw resistance. This research not only achieves the high - value utilization of waste foam concrete and reduces environmental pollution, but also provides technical support for improving the long - term performance of gravel soil subgrades in cold regions.

Author Contribution: Jizhong Gan: Conceptualization, Formal analysis, Writing, Investigation. XianTao Liang: Conceptualization, Formal analysis. Yang Song: Conceptualization, Formal analysis. Bingxu Chen: Methodology, Data curation, Writing -original draft, Visualization, Writing - review & editing. Dongsheng Liu: Conceptualization, Formal analysis, Investigation, Writing -review & editing. Wanzhi Cao: Conceptualization, Formal analysis, Investigation. Danhua Chen: Conceptualization, Formal analysis.

Acknowledgments: The authors would like to thank the financial support from the Gansu Provincial Natural Science Foundation (26JRRA374); Scientific Research Project of Talent Introduction in Northwest Minzu University (xbmuyjrc2023019); Central Universities Double Carbon Technology Innovation Research Project (3192024053 and 319024056); Gansu Provincial Department of Education: Major Cultivation Project for University Research and Innovation Platform (2024CXPT-19);The Gansu Provincial Key Science and Technology Special Plan Project(2025GZ029); The Gansu Provincial Key Science and Technology Special Plan Project Project Name: Technology Achievement Transformation Project for Resource Utilization of Coal Gangue in Preparing High-Activity, Low-Carbon and Ecological Cementitious Materials(2025GZ029).

References

1. ZHAO M Z, LIU G, DENG L X, et al. Optimizing the compaction characteristics and strength properties of gravelly soils in terms of fine contents[J]. *Advances in Materials Science and Engineering*, 2021, 2021: 6634237.
2. WANG T, YUE Z R. Influence of fines content on frost heaving properties of coarse grained soil[J]. *Rock and Soil Mechanics*, 2013, 34(2): 359–363.
3. PASTOR J L, CHAI J, SÁNCHEZ I. Strength and microstructure of a clayey soil stabilized with natural stone industry waste and lime or cement[J]. *Applied Sciences*, 2023, 13(4): 2583.
4. ONYELOWE K C, MOGHAL A A B, EBID A, et al. Estimating the strength of soil stabilized with cement and lime at optimal compaction using ensemble-based multiple machine learning[J]. *Scientific Reports*, 2024, 14(1): 15308.
5. ZHUANG S, XIE H, LING J. Study on the performance of cement-lime stabilized soil for road subgrade[J]. *Journal of Highway and Transportation Research and Development*, 2001, 18(3): 25–29.
6. BOAVENTURA N F, SOUSA T F D P, CASAGRANDE M D T. The application of an eco-friendly synthetic polymer as a sandy soil stabilizer[J]. *Polymers*, 2023, 15(24): 4626.
7. LI H, JIA J, LU X, et al. The effect of ionic soil stabilizer on cement and cement-stabilized iron tailings soil: Hydration difference and mechanical properties[J]. *Materials*, 2025, 18(7): 1444.
8. WU Y, LIU X, YANG J, et al. Influence of the wide range cement content on the properties of cement-treated marine soft soil and bound method of semi-solidified soil[J]. *Case Studies in Construction Materials*, 2024, 20: 03180.
9. WANG J, LI X, WEN H. Shrinkage cracking model for cementitiously stabilized layers for use in the mechanistic-empirical pavement design guide[J]. *Construction and Building Materials*, 2020, 260: 119–130.
10. SAHLABADI S H, BAYAT M, MOUSIVAND M, et al. Freeze-thaw durability of cement-stabilized soil reinforced with polypropylene/basalt fibers[J]. *Journal of Materials in Civil Engineering*, 2021, 33(9): 04021232.
11. SHIBI T, KAMEIT. Effect of freeze-thaw cycles on the strength and physical properties of cement-stabilised soil containing recycled bassanite and coal ash[J]. *Cold Regions Science and Technology*, 2014, 106: 36–45.
12. LAVEGLIA A, SAMBATARO L, UKRAINCZYK N, et al. Hydrated lime life-cycle assessment: Current and future scenarios in four EU countries[J]. *Journal of Cleaner Production*, 2022, 369: 133224.
13. KOGBARA R B, MASAD E A, LITTLE D N, et al. A state-of-the-art review of polymers used in soil stabilization[J]. *Construction and Building Materials*, 2021, 305: 124685.
14. LIU Y, ZHAO Z, AMIN M N, et al. Foam concrete for lightweight construction applications: A comprehensive review of the research development and material characteristics[J]. *Reviews on Advanced Materials Science*, 2024, 63(1): 20240022.
15. LIU J, LIU Y, MA X, et al. Thermal performance optimisation of foam concrete for energy-efficient construction: A state-of-the-art review[J]. *Journal of Building Engineering*, 2025, 113899.

16. FU Y, WANG X, WANG L, et al. Foam concrete: a state-of-the-art and state-of-the-practice review[J]. *Advances in Materials Science and Engineering*, 2020, 2020: 6153602.
17. JUST A, MIDDENDORF B. Microstructure of high-strength foam concrete[J]. *Materials Characterization*, 2009, 60(7): 741–748.
18. HUANG W, LIU J, SHI Q, et al. Mechanical and pore properties of foam concrete under salt erosion environment[J]. *Materials*, 2025, 18: 2810.
19. HUANG B, WANG X, KUA H W, et al. Construction and demolition waste management: China's lessons[J]. *Resources, Conservation and Recycling*, 2018, 129: 36–44.
20. ENGELSEN C J, VAN DER SLOOT H A, PETKOVIC G. Leaching behaviour of recycled aggregate used in unbound road layers—A laboratory study[J]. *Waste Management*, 2017, 61: 408–416.
21. WEBER R, MÜLLER J. Landfilling of construction and demolition waste: A review of environmental issues[J]. *Waste Management & Research*, 2013, 31(10): 1005–1016.
22. ZUHEIR B, AL-MULALIM Z. An innovative approach on recycle foam concrete as a sustainable alternative with the addition of nano titanium dioxide TiO₂ on the properties of foam concrete[J]. *Engineering, Technology & Applied Science Research*, 2025, 15(1): 19196–19199.
23. TURKEY F A, BEDDU S, AL-HUBBOUBI S K, et al. Recycled foam concrete masonry and porcelanite rocks-based lightweight geo-polymer concrete at elevated temperatures[J]. *Alexandria Engineering Journal*, 2024, 105: 171–180.
24. ZUHAIR B, AMEER M Z A. Innovative approach to foam concrete production by utilizing recycled foam concrete as a sustainable alternative[J]. *Journal of Engineering*, 2025, 31(4): 159–174.
25. GOŁASZEWSKI J, CYGAN G, GOŁASZEWSKA M, et al. Utilization of recycled foam concrete powder with phase-change material as a cement or sand replacement: Impact on mortar properties and superplasticizer performance[J]. *Sustainability*, 2025, 18(2): 1004.
26. SONG Y, LANGE D. Crushing performance of ultra-lightweight foam concrete with fine particle inclusions[J]. *Applied Sciences*, 2019, 9(5): 876.
27. PIZOŃ J. Fresh, mechanical, and thermal properties of cement composites containing recycled foam concrete as partial replacement of cement and fine aggregate[J]. *Materials*, 2023, 16(22): 7169.
28. OHEMENG E A, EKOLU S O. A review on the reactivation of hardened cement paste and treatment of recycled aggregates[J]. *Magazine of Concrete Research*, 2020, 72(10): 526–539.
29. CUNHA S, KAPTAN K, HARDY E, et al. Assessment of the efficiency of mechanical grinding and calcination processes for construction and demolition waste as binder replacement in cement pastes: Mechanical properties evaluation[J]. *Sustainability*, 2025, 17: 5248.
30. STEPKOWSKA E T, BLANES J M, FRANCO F, et al. Phase transformation on heating of an aged cement paste[J]. *Thermochimica Acta*, 2004, 420(1-2): 79–87.
31. JI X, JI D, YANG Z, et al. Study on the phase composition and structure of hardened cement paste during heat treatment[J]. *Construction and Building Materials*, 2021, 310: 125267.
32. HASANIN T H A, ALSAHLI S A, ALTALLEB H A, et al. Hydration characteristics of cement blended with thermally reactivated recycled concrete demolition waste[J]. *Scientific Reports*, 2026, 16: 1499.
33. XI X, ZHENG Y, DU C, et al. Study on the hydration characteristics, mechanical properties, and microstructure of thermally activated low-carbon recycled cement[J]. *Construction and Building Materials*, 2024, 447: 138042.
34. XU R, XIE Y, CHEN Y, et al. Mechanical properties and micro-mechanisms of soft soil stabilized with rice husk ash and multi-source solid waste-based cementitious materials[J]. *Frontiers in Built Environment*, 2025, 11: 1759978.
35. ZHUANG S, WANG Q, LUO T. Effect of C₁₂A₇ in steel slag on the early-age hydration of cement[J]. *Cement and Concrete Research*, 2022, 162: 107010.
36. JIANG N, WANG C, WANG Z, et al. Strength characteristics and microstructure of cement stabilized soft soil admixed with silica fume[J]. *Materials*, 2021, 14(8): 1929.
37. LAI Z, CHEN Y. Enhancing the mechanical and environmental performance of solidified soil using construction waste and glass micro-powder[J]. *Heliyon*, 2024, 10(22): e40187

38. ZHANG W, MU F Y, XUE Q, et al. Solidification/stabilization mechanisms of uncalcined waste concrete powder and ground granulated blast slag on lead-contaminated soil: From nanoscale to macroscale[J]. *Journal of Environmental Chemical Engineering*, 2025, 13(5): 117776.
39. TIAN H, WEI C, TAN L. Effect of freezing-thawing cycles on the microstructure of soils: A two-dimensional NMR relaxation analysis[J]. *Cold Regions Science and Technology*, 2019, 158: 106–116.
40. REN H, ZHANG D, ZHANG L, et al. Research advances in the freeze–thaw resistance of cement-stabilized soils[J]. *Journal of Cold Regions Engineering*, 2026, 40(2): 03126001.

Disclaimer/Publisher’s Note: The statements, opinions and data contained in all publications are solely those of the individual author(s) and contributor(s) and not of MDPI and/or the editor(s). MDPI and/or the editor(s) disclaim responsibility for any injury to people or property resulting from any ideas, methods, instructions or products referred to in the content.